

Analytical modeling of fracture energy with cohesion effects based on experimental investigations

Amina Benguelil^{*,1,a}, Brahim Elkhail Hachi^{1,b}, Mohamed Haboussi^{2,c}

¹Laboratory of Development in Mechanics and Materials (LDMM), University of Djelfa, Algeria

²Process and Materials Sciences laboratory (LSPM) Sorbonne Paris Nord University, France

Article Info

Abstract

Article history:

Received 03 Sep 2024

Accepted 12 Nov 2024

Keywords:

Concrete;

Experimental

investigation;

Fracture energy;

Analytical modeling;

Sand fines ratio;

Crack initial length

The experimental characterization is the most exact method which describes and studies the material's real behavior and its response to different mechanical solicitations otherwise conducting experimental tests for every case is often impractical. This work presents an analytical model that describes the concrete fracture energy variation in function of the specimen's length, the crack initial length and the Sand fines ratio basing on experimental investigations. Three point bending tests were conducting on concrete specimens, using an MTS testing machine and according to the ASTM norms. The obtained experimental results were used to generate an analytical model based on ANOVA and experimental plan principles. The model was validated and adjusted. It has been found that the weakening of the studied specimens is majorly related to the increasing on the specimen's and crack initial lengths or by decreasing the sand fines ratio and the model shows in addition to that a clear parameter's classification, the sand fines ratio is the most influential factor and all the interactions including the sand fines ratio or the crack initial length present high effects. A high coherence between the model and the experimental values in term of fracture energy was noticed and that according to relative error that did not exceed the 28%. After adjustments, the error was highly ameliorated. The model helps in studying the concrete general behavior and offers a reliable tool contributing to the evaluation of the Fracture energy without going through experimental tests considered as costly in terms of time and price.

© 2024 MIM Research Group. All rights reserved.

1. Introduction

Understanding the relationships between the microstructural phenomena and the corresponding effects on macroscopic behavior is the main key to truly understanding the material general behavior and the principal way to the establishment of the predictive formulate models for large-scale structural performance and reliability [1]. This relation's complexity depends mainly on the material sensibility, the confounding effects of design, the imposed loads, and the climatic conditions relevant to the structures [2]. The general theory of material behavior develops systematic methods to represent material properties in a context of physical evidence and mathematical consistency [3]. The Fracture mechanics is a field that uses the fracture phenomena and parameters to develop predictive models. It is the discipline of mechanics that deals with the study of the cracks propagation in materials due to the extension of processing defects such as pores, inclusions, or even microscopic fissures. It uses analytical methods known as analytical solid mechanics to calculate the driving force on cracks and applies the experimental solid mechanics principals to characterize the material's resistance to fracture. The Materials

*Corresponding author: amina.benguelil@univ-djelfa.dz

^aorcid.org/0009-0005-4588-1272; ^borcid.org/0000-0002-6672-746X; ^corcid.org/0000-0001-8901-6559

DOI: <http://dx.doi.org/10.17515/resm2024.431me0903rs>

Res. Eng. Struct. Mat. Vol. x Iss. x (xxxx) xx-xx

fracture behavior can be classified in ductile and fragile, where the fragile behavior is considered hard to detect and to study for the reason that the fracture is brusque, happens in a very quick manner and the materials engendering these type of behavior are very sensitive to the smallest changes in the study parameters or in the testing procedures. Concrete is one of the most well-known and highly used materials engendering these quasi-brittle behavior and because of its importance as a construction material, its fracture and failure behavior has been the subject of extensive researches [4], these researches has started in the 19th and the first half of the 20th where the demand for the concrete use has raised, these researches were focused on the concrete technology and its structural performances and lays majorly on the fracture and failure concrete behavior studies both experimental and numerical. The experimental investigations were divided on two main research axes, the investigations in term of concrete composition and nuances in a hand and on the material characterization and detection of their fracture parameters on the other one. To finally confuse these two axes in order to detected the optimum version of concrete to be used in different constructions sectors or to develop analytical predictive models that facilitate and helps in studying the concrete behavior without the need for experimental realizations. Focusing on the fracture energy predictive models based on experimental investigations were conducted such those presented by Bazant and Oh [5], proposing a model that links the said energy to the tensile strength, the aggregates diameter and the elasticity modulus, this model was simplified and reformulate later. Or the one developed by Hillerborg [6] based majorly on the area under the softening phase of the stress-strain curve obtained from bending test and takes also in consideration geometric parameters such as the crack length and the specimen's width. Meanwhile, the comite Euro International du béton [7] propose a simple empirical model defines the fracture energy in function of the aggregate maximum size and the cylinder compressive strength. This model was reformulated by Bazant et al. [8] and that by adding the water cement ratio. Years later, the Comite International du Béton [9] has proposed another model based on the mean value of the cylinder compressive strength. The JSCE [10] introduce as well a simplify model that contains only the aggregate maximum diameter and the cylinder compressive strength. Iman M.Nikbin et al. [11] propose a new model that takes in account the cylinder compressive strength, the concrete age and the water cement ratio. Others has proposed models based purely on numerical approaches and investigations such those conducted by Al-Saawani.M.A et al[12] who propose a model based on the Finite Element Modeling principals or even those based on cohesive approaches [13-17]. After analyzing the presented above models, it has been noticed that the generated models converge to the real behavior of concrete when more experimental parameters are taken into account. For that a lot of experimental works and researches highlighted the fracture parameters and their interchangeability with the specimen's size [18-27]. others present the concrete components impacts precisely the sand type and conclude that the sand grains shape, size and distribution can highly effect these fracture proprieties [28-32]. For our case, we are focused on three parameters which are the specimen's length, the crack initial length and the sand fines ratio considered as important and non-conventional factors. However, no model in literature (in our knowledge) has generated a relation between the fracture energy and these parameters in a hand neither define their interactions in the same model on the other one. Therefore, the present work came in the context of presenting a new analytical predictive model that defines the fracture energy in function of the mentioned above parameters and interaction's effect. It contains only experimental parameters. The model was elaborated based on experimental investigation results treated with on ANOVA and experimental Plan principles. The Database was extracted from three point bending testes done on concrete specimens through an MTS testing machine according to the ASTM norms. Studying and highlighting the effect of the specimen's length, the crack initial length and the sand classification was

extracted from the model and validated experimentally. By defining a relationship between the fracture energy and the experimental studied parameters, this works contribute on the concrete failure behavior studies as it can be used for numerical application.

2. Materials and Methods

2.1. Specimen's Geometry and Characteristics

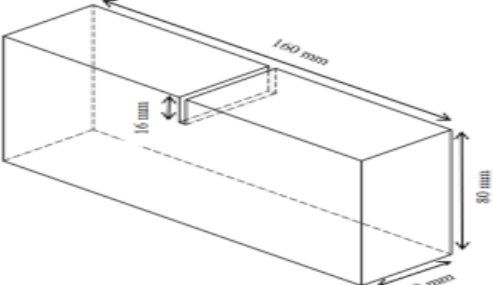
The experimental approach of the present study is carried out in a context following the standard experimental procedures of engineering, such as those described in [33; 34]. We present here several parametric studies, where three different values for each factor were tested experimentally. All this configurations' sizes were realized according to the ASTM Norms particularly the ASTM C192/192M [35] dealing with the Standard Practice for Making and Curing Concrete Test Specimens in the Laboratory, the chosen specimens are all rectangular in shape and having the dimensions and characteristic recapitulated as follow:

2.1.1 The Specimen's Length

The tested specimen's length configurations are shown in Table 1.

Table 1. The tested specimen's lengths

The specimen's length
$S_l=160$ mm
$S_l=180$ mm
$S_l=200$ mm

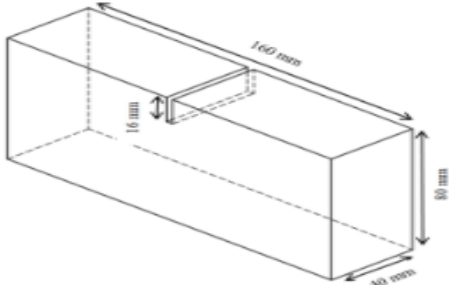


2.1.2 The Crack Initial Length

The tested crack initial length values are shown in the table below, and their size was kept as 160 x 80 x 40 mm:

Table 2. The crack initial lengths

The crack initial lengths
$C_l=1,6$ mm
$C_l=1,8$ mm
$C_l=2$ mm

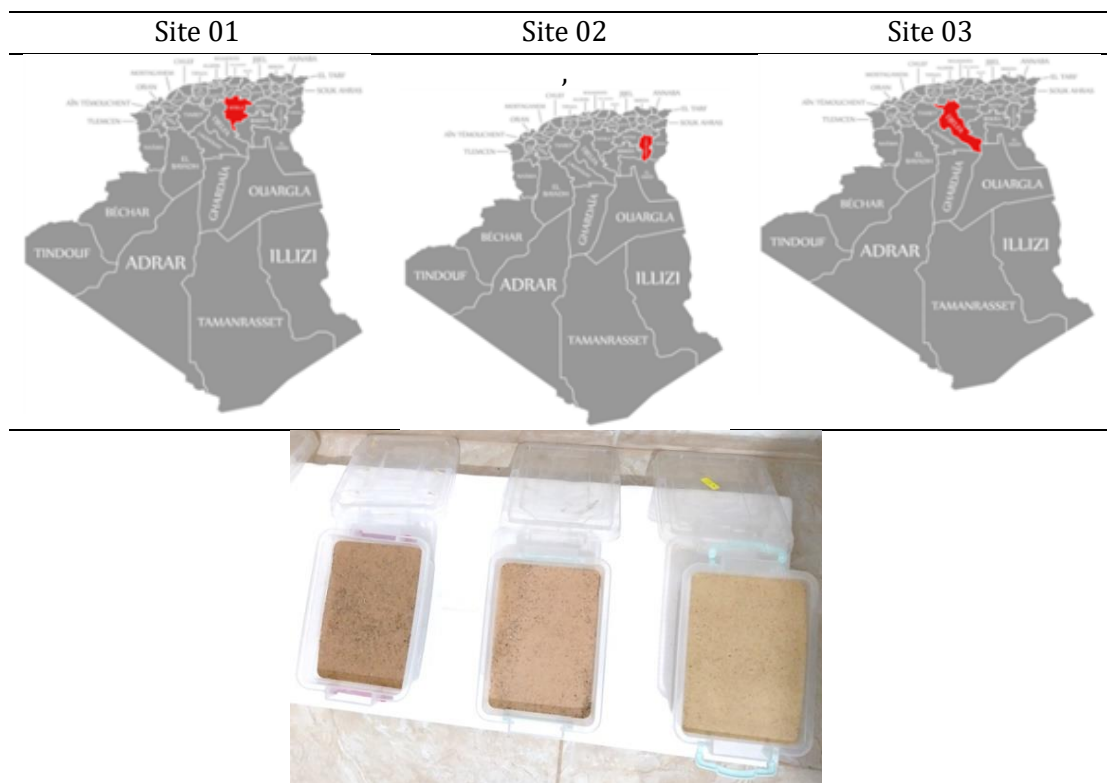


2.1.3 The Sand Type

This part deals with the Sand Class influence, where three different classes of sand were tested. Each class was firstly characterizing in term of chemical and granulometric composition. All the obtained tests are presented above:

- Site 01: From the Algerian center precisely the city of M'sila, the first class of samples was chosen.
- Site 02: from the Algerian East precisely the city of Khenchela, the second class of samples was chosen.
- Site 03: From the Algerian middle-south precisely the city of Djelfa, the third class of samples was chosen. The sand's type localization is presented on Table 3.

Table 3. The sand samples localization



The sand samples chemical examinations have been done on laboratories specialized in sand characterization and engenders the results presenting in Table 4:

Table 4. The sand chemical compositions

Compositions (%)	Site 01	Site 02	Site 03
SiO ₂	92,52	94,26	89,17
Al ₂ O ₃	0,54	2,04	1,21
Fe ₂ O ₃	0,27	0,39	0,70
CaO	3,12	1,09	4,12
MgO	0,03	0,00	0,12
SO ₃	0,14	0,08	0,05
K ₂ O	0,22	0,89	0,41
Na ₂ O	0,01	0,23	0,01
P ₂ O ₅	0,01	0,01	0,01
TiO ₂	0,11	0,06	0,15
MnO	0,01	0,01	0,01

For the Granulometric examinations have given the results presenting in Table 5:

Table 5. The Granulometric analysis results.

Sand class	Sand Fines ratio	% Sieve /0,65μm
Site 01	1,44	1,2
Site 02	1,62	1,8
Site 03	1,86	2,6

2.2 Materials and Specimen Preparations

In this study, all specimens had been manufactured with a similar concrete mixture and procedure and that according to the ASTM C192/C192M. The main conditions imposed by this Norm and applied in our specimen’s preparation can be recapitulated as follows:

- The components must be cleaned, sifted, dried and brought to a room with a temperature range of 68 to 86°F (20 to 30°C) and that even before mixing the concrete;
- The specimen molds must be installed on a rigid surface free from vibration or any other disturbances and as close as possible to the location where they will be stored for their first 24 hours. For Reusable molds, they shall be lightly coated with mineral oil or a suitable nonreactive release material before use;
- The Hand-mixed batches of concrete must be prepared in a manner that an amount of 10% will be remain as excess flow after filling the molds;
- Mix both fine and coarse aggregates with dry cement until they are thoroughly blended and the aggregates are uniformly distributed throughout the batches and that before adding the water;
- Adding water and mixing the mass until the concrete is homogeneous in appearance and has the desired consistency;
- Cover the mixed concrete in order to prevent evaporation during the specimen’s full in procedure;
- Place the concrete in the molds using a scoop or a shovel; and genuinely tapping the mixture and highly vibrate the molds in order to release the extra water and to minimize as possible the air bulbs containing inside the specimen’s
- The molds shall be left to dry at least for 24 Hours before getting storage.
- The specimens must be storage in a dry, free from humidity, clean from dust spaces and preferably in storage containers before carrying the tests (they must be stored at least for at least 28 days for flexural tests).

For the concrete tested mixture components and proportions, they are recapitulated in Table 6:

Table 6. Concrete Component’s proportions.

Mixture	Values
Cement-Sand ratio (C/S)	1,11
Water-Cement ratio (W/C)	0,89
Cement (kg)	0.134
Fine aggregate 3-8 (kg)	0.515
Sand (kg)	0.429
Water (liter)	0.12

The specimen’s preparation is recapitulated on the following steps:

- The specimens were realized via a normalized Wood Molds that ensures the fabrication of four specimens at time. The molds are lightly coated by a nonreactive burn oil before pouring the concrete mixture, as shown in Figures:



Fig. 1. The Wood Molds

- The components were cleaned, sifted and dried and measured according to the specimens' proportions, as shown in Figures:



Fig. 2. The components storage before mixing

- The measured components were mixed according to the ASTM C192/C192M, were the aggregates and the cement were well mixed before adding the sand and the water. The final mixture was also genuinely mixed and that in order to get an homogeneous concrete with the desired consistency, the obtained mix is shown in the picture below:

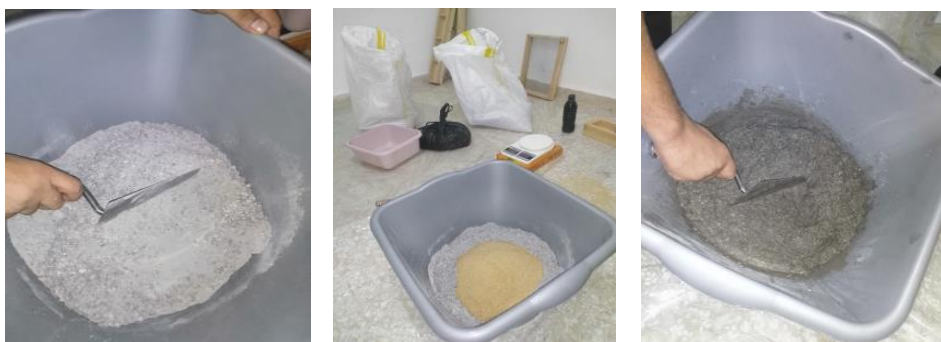


Fig. 3. The concrete mixture

- The concrete was pouring to the molds as required on the followed norm and the obtained specimens are shown in the Figure below:



Fig. 4. The specimen's concrete pouring

- The specimens were finely storage in a dry and free from dust and humidity space before transformed to the laboratory where they will be storage until the test curing.



Fig. 5. The specimen's storage

NB: it is to be mentioned that all the tests were applied on specimen's aging more than 28 days.

2.3 Experimental Procedures

The conducting experiments were a three point bending tests done according to the ASTM C293/C293M [36] and performed using an MTS testing machine one of the most efficient and well-known testing machine on the experimental fields. This testing machine uses a hydraulic system in the Crossbars displacement control the thing that offers a high stability during test, when applying small speeds, high loads or even while testing big specimens. The test curing can be controlled either manually through the control handle or automatically through the MPE software assistance. When choosing the automatically controlled tests, the MTS machine offers to users the possibility of generating their own procedure. The maximum loading can achieve a 100KN and the test can take even two hours of timing the thing that presents a high precision and detection of the smallest phenomenon that can appears during the tests. The results are also automatically generated through a data base acquisition system installed on the used software. Our tests were controlled by displacement and that for all specimens. Applying a constant displacement of 0.2 mm/min for almost an hour and fifteen (15) min ensure a high detection and precision of the obtained results. During the tests, the applied load and

displacement were simultaneously recorded. Once the tests are finished, all the selected signals were outputted for treatment through a dynamic data acquisition system, the following Work chart presents the procedure applied during these tests:

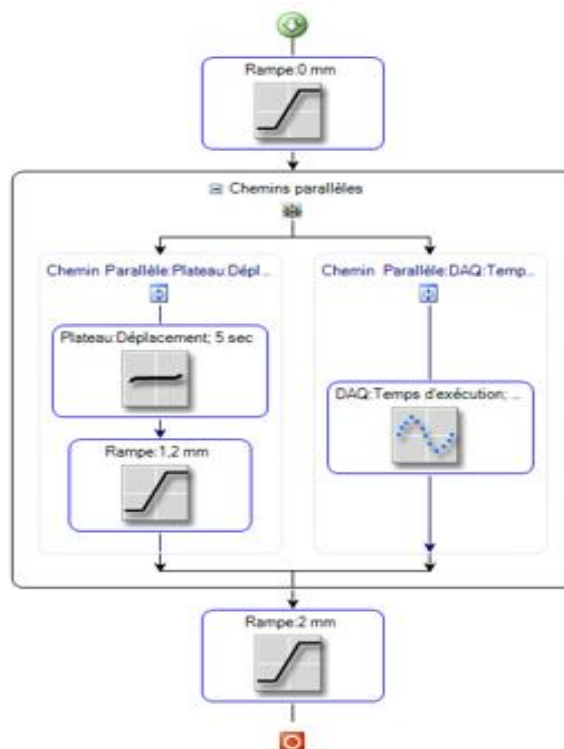


Fig. 6. The applied procedure

According to the presented above work chart, the procedure steps can be recapitulated as follow:

- Step 0: a Ramp that ensure the placement of lower Crossbars in an initial position of zero (0 mm) coordinate;
- Step 1: maintaining the lower Crossbars on obtained position from Step 0 for stabilizing the tested specimens.
- Step 2: Applying a constant Ramp to ensure a displacement from the stabilization position (0mm) to a - 1,2 mm (this position was determined after curing initial tests until defining the displacement generating the crack phenomenon and then using this value in the automatic procedure). The tests will be curing almost for an hour and fifteen min the thing that generate a tests speed equal to 0,2 mm/min (optimal speed for a stable and precise tests);
- Step 3: Releasing the cracked specimens by defining a Ramp displacement of 2 mm adequate for extracting the tested specimen.

For the testing specimen's set-up, it was done as clarified in the (ASTM C293/C293M) norms, knowing as "Standard Test Method for Flexural Strength of Concrete (Using Simple Beam with Center-Point Loading)". The tested specimens were installed on the MTS testing features according to the presented above installation norm and in accordance with the testing machine specifications, as shown in the Figure 8.

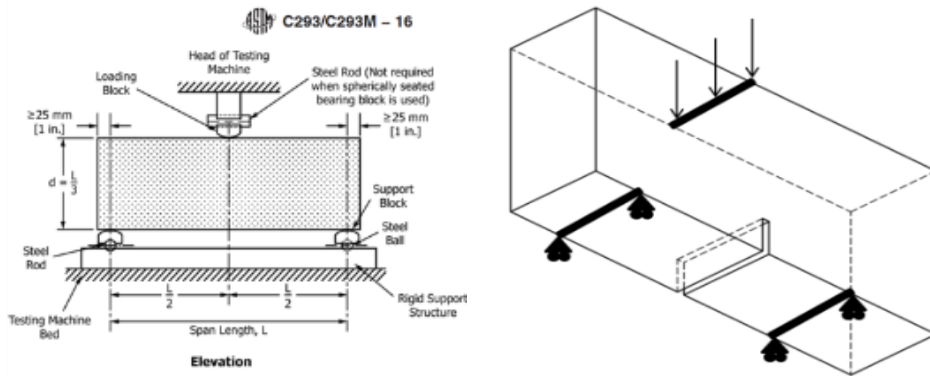


Fig. 7. The ASTM C293 three point bending tests set-up



Fig. 8. The ASTM C192 testing set-up

2.4 Experimental Results

This section includes all the obtained results, starting from the Load-Deflection curves, the parametric study results and the factors effects on the studied Fracture Energy.

- The Load-Deflection curves of the tested specimens are presented below:

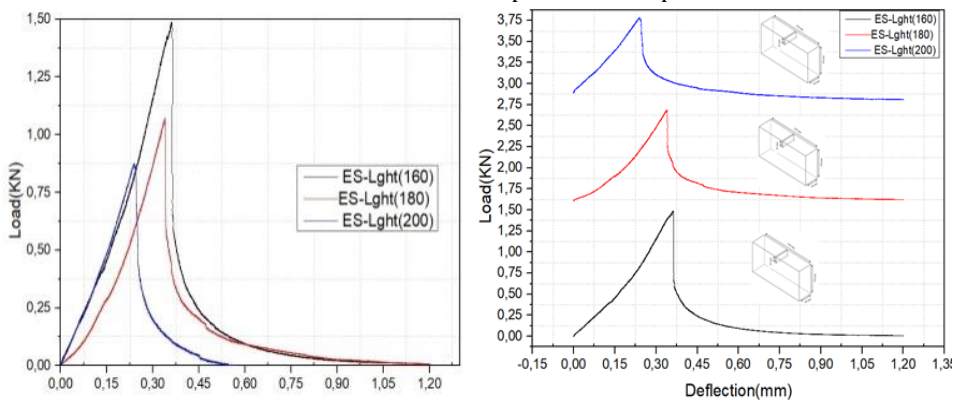


Fig. 9. Load-Deflection curve of the studied specimen's lengths

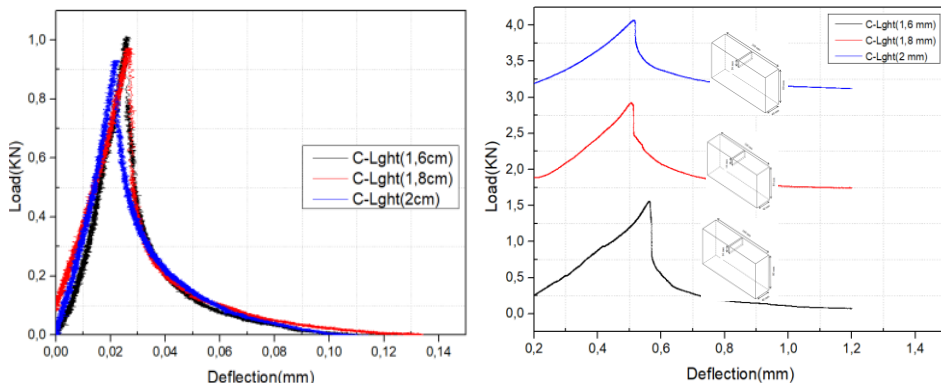


Fig. 10. Load-Deflection curve of the studied crack initial lengths

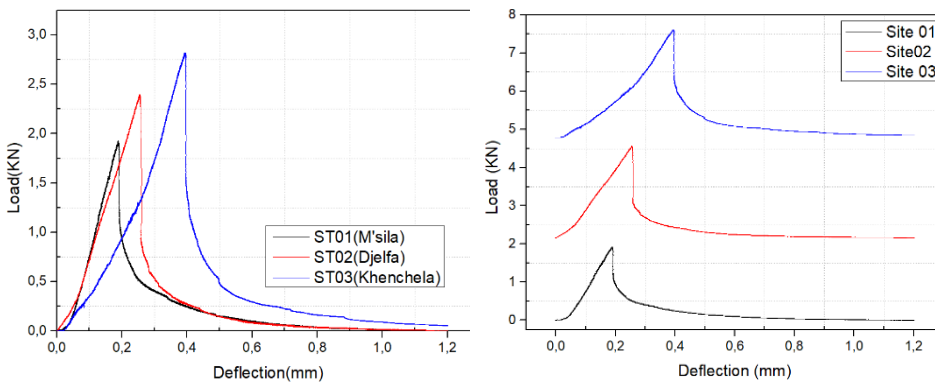


Fig. 11. Load-Deflection curve of the studied and classes

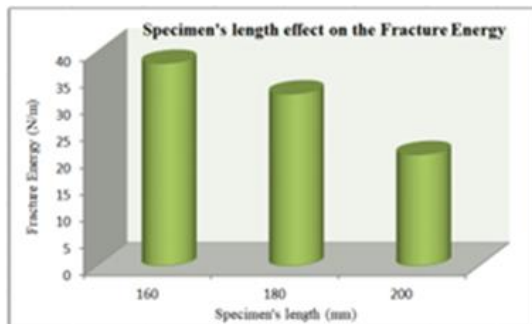
The Tables 7-9 recapitulates the fracture energies, the maximum deflections and the peak loadings for each factor and each configuration:

- The specimen's length effect on the fracture energy

The specimen's length effect on the fracture energy is presented on the Table 7:

Table 7. The specimen's length configurations

Factor	Values(mm)	P_l (KN)	$d_x \cdot 10^{-2}$ (mm)	G_f (GPA)
S_l	160	1,5	4,512	37,71
	180	1	4,051	32,03
	200	0,8	3,849	20,72

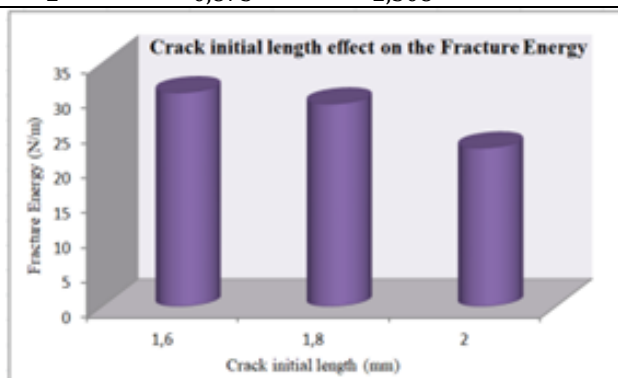


- The crack initial length effect on the fracture energy:

In Table 8, all the obtained results concerning the crack initial length effect on the fracture energy were presented:

Table 8. The Crack initial length configurations

Factor	Values	P_l (KN)	$d_x 10^{-2}$ (mm)	G_f (GPA)
C_l	1,6	1,013	2,228	30,64
	1,8	0,932	1,937	29,03
	2	0,875	2,308	22,71

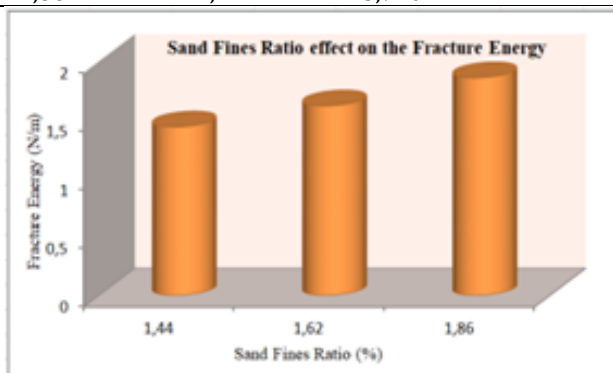


- The Sand Fines Ratio effect on the fracture energy:

The Table 9 shows the Sand fines Ratio effect on the fracture energy:

Table 9. The Sand fines ratio configuration

Factor	Values	P_l (KN)	$d_x 10^{-2}$ (mm)	G_f (GPA)
S_R	1,44	2	1,797	41,87
	1,62	2,4	2,480	45,59
	1,86	2,7	3,940	50,32



2.5 Results Discussion

For each studied parameter and configuration, the load-Deflection curves were plotted, the load maximum Deflection and the peak loading were extracted and the fracture energies were calculated. In a general contest, the presented curves were satisfying and representative; they reflect the reel behavior of concrete. The obtained results are recapitulated as follow:

- Specimen’s length results: According to the presented curves and the recorded values, the fracture energies and peak loading increase while decreasing the specimen’s lengths. Thus, we conclude that the augmentation on the specimen’s length reduces the required energy to break it and the fracture phenomenon happens earlier.
- Crack initial length results: for this factor it has been noticed that the augmentation of the initial crack length engenders a considerable decreasing on the maximum deflection and on the fracture, energy required to generate the specimen’s failure and that was clearly noticed on the fracture energy variation in function of the crack initial length. This means that the specimen’s fragility depends on the crack initial length in a very considerable manner. During the bending tests a group of micro-fissures happens and their branching engenders the crack. The resultant fissure propagates where it dissipates the lower energy so it goes to the initial crack and more its initial length is bigger more it favors the specimen’s failure.
- The Sand Fines Ratio results: For the sand classification and after presenting both chemical and Granulometric analysis, it has been noticed that the three samples differ majorly on their fines Ratio. This parameter has generated the results the most interesting and that because its impact was clearly appearing on both the maximum loading and the deflection causing the specimen’s failure in a very considerable manner comparing to the two other parameters. The Load deflection curves show the high sensitivity of the concrete peak loading and maximum deflection to the smallest variation on the fine’s ratio values. For the fracture energy histograms, the sand fines ratio augmentation engenders a considerable increase on the fracture values. This can be explained by the fact that the increasing on this Ratio increases also the mixture heterogeneity, so it makes the concrete mixture more consistent and augments its cohesion propriety.

3. Mathematical Modeling

The main objective through this section is the elaboration of an analytical model that illustrates and defines the variation of the fracture energy in term of specimen’s length, crack initial length and the sand fines ratio. The model is elaborated based on experimental results and statistical methods [36]. In our case, we applied the ANOVA analysis combined with the experimental plan principles. The main steps of the model elaboration are presented below:

- Step I: before elaborating the model, it is necessary to extract experimental tests that illustrate all the possible cases and probabilities of the studied factors the thing that highlights in this case 27 tests recapitulated and presented in the Table 10:

Table 10. Experimental tests

Tests	S_R	S_l	C_l	G_f
ES-001	1,44	0,16	1,6	31,85
ES-002			1,8	28,23
ES-003			2	25,93
ES-004		0,18	1,6	27,35
ES-005			1,8	25,5
ES-006			2	24,73
ES-007		0,2	1,6	23,03
ES-008			1,8	22,53
ES-009			2	20,34
ES-001	1,62	0,16	1,6	61,17

ES-002			1,8	58,78
ES-003			2	57,69
ES-004			1,6	46,73
ES-005		0,18	1,8	46,46
ES-006			2	41,66
ES-007			1,6	38,54
ES-008		0,2	1,8	35,06
ES-009			2	34,15
ES-001			1,6	73,3
ES-002		0,16	1,8	73,3
ES-003			2	71,72
ES-004	1,82		1,6	67,91
ES-005		0,18	1,8	66,73
ES-006			2	64,67
ES-007			1,6	63,23
ES-008		0,2	1,8	62,45
ES-009			2	61,1

- **Step II:** the choice of the significant tests, some tests must be eliminated and that for increasing the model precision and eliminating the repetitions. The Table 11 recapitulates the chosen tests and their codification using ANOVA codes:

Table 11. The significant coded tests

Tests	S_R	S_I	C_I	$S_R * S_I$	$S_R * C_I$	$S_I * C_I$	$S_R * S_I * C_I$	G_f
ES-001	-1	-1	-1	1	1	1	-1	35,06
ES-002	-1	-1	1	1	-1	-1	1	38,54
ES-003	-1	1	-1	-1	1	-1	1	41,66
ES-004	-1	1	1	-1	-1	1	-1	50,15
ES-005	1	-1	-1	-1	-1	1	1	57,69
ES-006	1	-1	1	-1	1	-1	-1	61,1
ES-007	1	1	-1	1	-1	-1	-1	62,45
ES-008	1	1	1	1	1	1	1	64,67

It is to be clarified that the “-1” refers to the lowest value in the factors levels: the “1” refers to the highest one and the “0” code refers to the medium value.

- **Step III:** Finally, the model is obtained using the Rechtschaffner modeling method [38], as presented below:

$$G_f = a_0 + \sum a_i * X_i + \sum a_{ij} * X_i * X_j \tag{1}$$

After developing the Rechtschaffner approach we obtain the following equation:

$$G_f = a_0 + a_1 * X_1 + a_2 * X_2 + a_3 * X_3 + a_{12} * X_{12} + a_{13} * X_{13} + a_{23} * X_{23} + a_{123} * X_{123} + e \tag{2}$$

- **Step IV:** Using ANOVA calculation and the Rechtschaffner modeling method, the model coefficients, presented in Table 12:

Table 12. The model coefficients

Coefficients	a_0	a_1	a_2	a_3	a_{12}	a_{13}	a_{23}	a_{123}
Values	/	21,05	4,39	1,54	0,78	0,32	0,29	0,47

The final model is giving as the follows:

$$G_f = 21,05 * S_R - 4,39 * S_l - 1,54 * C_l - 0,78 * S_R * S_l + 0,32 * S_R * C_l + 0,29 * S_l * C_l - 0,47 * S_R * S_l * C_l + e \quad (3)$$

Where: G_f : the fracture energy, S_R ; the sand fines ratio, S_l : specimen's length, C_l : crack initial length,

The proposed model shows the variation of the fracture energy in function of Sand fines ratio, the crack initial length and the specimen's length and their interactions. It is to be mentioned that the e is the global error recorded between the model and the experimental values used to adjust the proposed model. According to the models elaborated based on experimental investigation through AVOVA methods, the coefficients of each parameter and each interactions combination refers to its influence degree. The sand fines ratio is the most influential parameters because it represents the highest factor in the model formulation followed by the crack initial length and the specimen's length. For the specimen's length and the crack initial length, they present an inversely proportional relation due to their negative coefficients. The sand fines ratio engenders a proportional relation with the fracture energy variation and that because it has a positive coefficient on the model formulation. This can be explained physically by the fact that by increasing the fineness of the sand grains, the contact surfaces between these grains and the binder in concrete mixtures (in our case the cement) increase, which inevitably increases the cohesion and therefore the toughness of the material. The model shows also that the interactions between the sand ratio and the crack initial length engender a considerable impact comparing to the other combinations.

4. Validation Tests

In order to validate the proposed model supplement experiments were done and a comparison between the obtained experimental results and the model values was done in term of fracture energy, the Table 12 presents all the details:

Table 12. The validation tests

N	S_R	S_l	C_l	Exp G_f	Model G_f	R-Error
1	1,44	0,16	1,6	31,85	32,4956864	2,03%
2	1,44	0,16	1,8	28,23	32,8834976	16,48%
3	1,44	0,16	2	25,93	33,2713088	28,31%
4	1,44	0,18	1,6	27,35	32,3730992	18,37%
5	1,44	0,18	1,8	31,89	32,7593808	2,73%
6	1,44	0,18	2	33,68	33,1456624	1,59%
7	1,44	0,2	1,6	30,17	32,250512	6,90%
8	1,44	0,2	1,8	31,25	32,635264	4,43%
9	1,44	0,2	2	33,17	33,020016	0,45%
10	1,62	0,16	1,6	37,71	36,3283112	3,66%
11	1,62	0,16	1,8	37,29	36,7249568	1,52%
12	1,62	0,16	2	42,69	37,1216024	13,04%
13	1,62	0,18	1,6	46,73	36,2001836	22,53%
14	1,62	0,18	1,8	46,46	36,5949594	21,23%

15	1,62	0,18	2	41,66	36,9897352	11,21%
16	1,62	0,2	1,6	38,54	36,072056	6,40%
17	1,62	0,2	1,8	35,06	36,464962	4,01%
18	1,62	0,2	2	34,15	36,857868	7,93%
19	1,82	0,16	1,6	41,66	40,5867832	2,58%
21	1,82	0,16	2	45,59	41,3997064	9,19%
24	1,82	0,18	2	50,51	41,2609272	18,31%
25	1,82	0,2	1,6	46,16	40,318216	12,66%
26	1,82	0,2	1,8	40,23	40,720182	1,22%
27	1,82	0,2	2	38,41	41,122148	7,06%

For the validation tests, a comparison between the experimental fracture energy and the one calculated through the model was done and the relative errors between the two values were also calculated. It was found that for any value of the sand fines ratio, the specimen's length or the crack initial length, the fracture energies extracted and calculated were very close and presents a high coherence with the experimental results. The recorded Relative errors were very acceptable, where the smallest value was 0,45% and the highest one was 28%, the thing that gives this model a high credibility and precession.

5. The Model Adjustment

After validating the model, we pass to the model adjustment using the error recorded during the validation. The error average is added to the proposed model and the new model will be compared once again to the experimental values. The new model became as follow:

$$G_f = 21,05 * S_R - 4,39 * S_l - 1,54 * C_l - 0,78 * S_R * S_l + 0,32 * S_R * C_l + 0,29 * S_l * C_l - 0,47 * S_R * S_l * C_l - 0,93 \quad (4)$$

The model adjustment results are presented in the Table 13:

Table 13. The validation tests

N	S_R	S_l	C_l	Exp G_f	Model G_f	R Error	New model	NR Error	Diff
1	1,44	0,16	1,6	31,85	32,4956864	2,03%	31,565686	0,89%	1,14%
2	1,44	0,16	1,8	28,23	32,8834976	16,48%	31,953498	13,19%	3,29%
3	1,44	0,16	2	25,93	33,2713088	28,31%	32,341309	24,73%	3,58%
4	1,44	0,18	1,6	27,35	32,3730992	18,37%	31,443099	14,97%	3,40%
5	1,44	0,18	1,8	31,89	32,7593808	2,73%	31,829381	0,19%	2,54%
6	1,44	0,18	2	33,68	33,1456624	1,59%	32,905662	2,30%	-0,71%
7	1,44	0,2	1,6	30,17	32,250512	6,90%	31,320512	3,81%	3,09%
8	1,44	0,2	1,8	31,25	32,635264	4,43%	31,705264	1,46%	2,97%
9	1,44	0,2	2	33,17	33,020016	0,45%	33,090016	0,24%	0,21%
10	1,62	0,16	1,6	37,71	36,3283112	3,66%	36,398311	3,48%	0,18%
11	1,62	0,16	1,8	37,29	36,7249568	1,52%	35,994957	3,47%	-1,95%
12	1,62	0,16	2	42,69	37,1216024	13,04%	36,191602	11,06%	1,98%

13	1,62	0,18	1,6	46,73	36,2001836	22,53%	36,270184	22,38%	0,15%
14	1,62	0,18	1,8	46,46	36,5949594	21,23%	35,664959	23,24%	-2,01%
15	1,62	0,18	2	41,66	36,9897352	11,21%	36,759735	11,76%	-0,55%
16	1,62	0,2	1,6	38,54	36,072056	6,40%	36,142056	6,22%	0,18%
17	1,62	0,2	1,8	35,06	36,464962	4,01%	35,534962	1,35%	2,66%
18	1,62	0,2	2	34,15	36,857868	7,93%	35,927868	5,21%	2,72%
19	1,82	0,16	1,6	41,66	40,5867832	2,58%	39,656783	4,81%	-2,23%
21	1,82	0,16	2	45,59	41,3997064	9,19%	41,163245	9,71%	-0,52%
24	1,82	0,18	2	50,51	41,2609272	18,31%	41,969706	16,91%	1,40%
25	1,82	0,2	1,6	46,16	40,318216	12,66%	41,922500	9,18%	3,48%
26	1,82	0,2	1,8	40,23	40,720182	1,22%	39,926713	0,75%	0,47%
27	1,82	0,2	2	38,41	41,122148	7,06%	40,330927	5,00%	2,06%

The model adjustment results show that by adding the average error to the elaborated model, the relative error has decrease considerably. The majority of the tested values had converged to the experimental ones and the new error did not exceed the 24%.

6. Conclusion

The main purpose through this work was the elaboration of an analytical model that defines the fracture energy in term of specimen's length, crack initial length and sand fines ratio and all their interaction probabilities based on experimental investigations. Based on three point bending tests through an MTS testing machine, ANOVA method and Experimental Plan principles the model was elaborated.

The experimental results can be recapitulated as follows:

- The specimen's length augmentation engenders a decrease on the fracture energy and the peak loading values.
- The crack initial length augmentation engenders a decrease on the fracture energy and the maximum deflection
- The augmentation of the sand fines ratio engenders a considerable increase on the fracture energy and presents a clear influence on both peak loading and maximum deflection point.

Concerning the modeling results, we can say that the elaborated model defines the fracture energy variation in function of the chosen parameters: the crack initial length, the specimen's length and sand fines ration and all their interaction probabilities. It shows according to ANOVA analysis that the sand fines ratio is the most influential factor and engender a proportional variation between the fracture energy and that because it has the highest coefficient in model formulation, followed by the crack initial length and finally the specimen's length. For the validation part, extra tests were done and that in order to compare the experimental fracture energy with the one calculated based on the elaborated model. A high coherence has been recorded between the two values and the recorded Relative Error doesn't exceed the 28%. These results give this model a high credibility and precession.

The elaboration of a mathematical model that engenders a relationship between the experimental parameters and the fracture energy is the main key to truly understand the concrete general behavior and a very efficient and precise manner to understand the corresponding effects engendering by the experimental or reel factors.

This model is considered as the only model that relay the fracture energy to the specimen's length, the crack initial length and the sand fines Ratio with all their interaction probabilities.

Finally, it should be mentioned that the present study can offer a reliable tool contributing to the evaluation of the energy of concrete failure for researchers and graduate students wishing to use this parameter in their modelling (particularly numerical) without going through experimental tests which can be costly in terms of time and price.

References

- [1] Aldahdooh MAA, Bunnori NM. Crack classification in reinforced concrete beams with varying thicknesses by mean of acoustic emission signal features. *Construction and Building Materials*. 2013;45: 282-288. <https://doi.org/10.1016/j.conbuildmat.2013.03.090>
- [2] Fronteddu L, Leger P, Tinawe R. The static and dynamic Static and Dynamic Behavior of Concrete Lift Joint Interfaces. *Journal of structural Engineering*. 1998;124(12). [https://doi.org/10.1061/\(ASCE\)0733-9445\(1998\)124:12\(1418\)](https://doi.org/10.1061/(ASCE)0733-9445(1998)124:12(1418))
- [3] Ibrahim M, Farhat M, Issa MA, Hass J. The Effect of Material Constituents on Mechanical and Fracture Mechanics Properties of Ultra-High-Performance Concrete. *ACI Materials Journal*. 2017; 114(03): 453-465. <https://doi.org/10.14359/51689717>
- [4] Landis EN. Micro-macro fracture relationships and acoustic emissions in concrete. *Construction and Building Materials*. 1999;13(1-2): 65-72. [https://doi.org/10.1016/S0950-0618\(99\)00009-4](https://doi.org/10.1016/S0950-0618(99)00009-4)
- [5] Bazant ZP, Oh BH. Crack band theory for fracture of concrete. *Materials and Structures*. 1983;16(03):155-177. <https://doi.org/10.1007/BF02486267>
- [6] Hillerborg A. The theoretical basis of a method to determine the fracture energy of concrete. *Materials and Structure*. 1985;18(4):291-296. <https://doi.org/10.1007/BF02472919>
- [7] Comité Euro-International du Béton. CEB-FIB Model Code 1990. Thomas Telford: Lausanne, Switzerland. 1993.
- [8] Bazan ZP. Concrete fracture models testing and practice. *Engineering Fracture Mechanics*. 2002;69(2):165-205. [https://doi.org/10.1016/S0013-7944\(01\)00084-4](https://doi.org/10.1016/S0013-7944(01)00084-4)
- [9] Comité Euro-International du Béton. CEB-FIB Model Code 1994. Thomas Telford: Lausanne, Switzerland. 1994
- [10] Japan Society of Civil Engineers. Standard Specifications for Concrete Structures 2007 "Design". 2007; 15:1-503.
- [11] Iman M, Nikbin SR, Allahyari H. A new empirical formula for prediction of fracture energy of concrete based on the artificial neural network. *Engineering Fracture Mechanics*. 2017;186 466-482. <https://doi.org/10.1016/j.engfracmech.2017.11.010>
- [12] Al-Saawani MA, Al-Negheimish AI, El-Sayed AK, Alhozaimy AM. Finite Element Modeling of Debonding Failures in FRP-Strengthened Concrete Beams Using Cohesive Zone Model. *Polymers*. 2022;14(9):1889. <https://doi.org/10.3390/polym14091889>
- [13] Alexandridis A, Gardner NJ. The cohesion behavior development in relation with the concrete freshness. *Cement and concrete Research*. 1981;11(3): 323-339. [https://doi.org/10.1016/0008-8846\(81\)90105-8](https://doi.org/10.1016/0008-8846(81)90105-8)
- [14] Boyu C, Hongfa Y, Jinhua Z, Haiyan M, Fangming T. Effects of the embedding of cohesive zone model on the mesoscopic fracture behavior of Concrete: A case study of uniaxial tension and compression tests. *Engineering failure analysis*. 2022;142:106709. <https://doi.org/10.1016/j.engfailanal.2022.106709>
- [15] De Maio U, Greco F, Leonetti L, Blasi P N, Pranno A. A cohesive fracture model for predicting crack spacing and crack width in reinforced concrete structures.

- Engineering Failure Analysis. 2022;139: 106452.
<https://doi.org/10.1016/j.engfailanal.2022.106452>
- [16] Haupt P. On the mathematical modeling of material behavior in continuum mechanics. *Acta Mechanica*. 1993;100: 129-154. <https://doi.org/10.1007/BF01174786>
- [17] Javanmardi MR, Maheri MR. Anisotropic Damage Plasticity Model for Concrete and Its Use in Plastic Hinge Relocation in RC Frames with FRP. *Structures*. 2017; 12: 212-226. <https://doi.org/10.1016/j.istruc.2017.09.009>
- [18] Ghasemi M, Ghasemi RM, Mousavi SR. The fracture parameters and size effect of steel fiber-reinforced self-compacting concrete. *Construction and Building Materials*. 2020; 201: 447-460. <https://doi.org/10.1016/j.conbuildmat.2018.12.172>
- [19] Hua R, Wei D, Bensheng Z. Size effect on fracture properties of concrete after sustained loading. *Materials and Structures*. 2019; 52:16. <https://doi.org/10.1617/s11527-019-1326-0>
- [20] Jirasek M, Rolshoven S, Grassl P. Size effect on fracture energy induced by non-locality. *Numerical and analytical methods in Geomechanics. Special Issue: Computational Mechanics of Concrete and Concrete Structures*. 2004;28: 653-670. <https://doi.org/10.1002/nag.364>
- [21] Karagari A, Akhaveissy AH, Pietruszczak S. The Experimental and meso-scale investigation of size effect on fracture properties in three-point concrete beams (TPB). *Theoretical and Applied Fracture Mechanics*. 2023; 127: 104026. <https://doi.org/10.1016/j.tafmec.2023.104026>
- [22] Ran Z, Syed YA, Loukili A. Experimental investigation on the correlation between the aggregate size effect and the structural size effect. *Engineering Fracture Mechanics*. 2020;234:107101. <https://doi.org/10.1016/j.engfracmech.2020.107101>
- [23] Scorza D, Ronchei C, Vantadori S, Zanichli A. The Size-effect independence of hybrid fiber-reinforced roller-compacted concrete fracture toughness. *Composites Part C: Open Access*. 2022; 9: 100306. <https://doi.org/10.1016/j.jcomc.2022.100306>
- [24] Yi C, Xiaozhi H. The interchangeability and selection of size effect and boundary effect experiments for characterization and prediction of quasi-brittle fracture of concrete. *Theoretical and Applied Fracture Mechanics*. 2020;122:103629. <https://doi.org/10.1016/j.tafmec.2022.103629>
- [25] Kai D, Xiaozhi H, Wittmann FH. Size effect on specific fracture energy of concrete. *Engineering Fracture Mechanics*. 2007; 4: 87-96. <https://doi.org/10.1016/j.engfracmech.2006.01.031>
- [26] Norashidah AR, Zainorizuan MJ, Zahir NNM. Fracture energy of foamed concrete by means of the three-point bending tests on notched beam specimens. *ARPN Journal of Engineering and Applied Sciences*. 2015;10(15):6562-6570.
- [27] Dubey S, Ray S. Influence of heterogeneity on size effect models and fracture characteristics of plain concrete. *Theoretical and Applied Fracture Mechanics*. 2023; 127: 103993. <https://doi.org/10.1016/j.tafmec.2023.103993>
- [28] Belhadj B, Bederina M, Benguetach KH, Queneude M. Effect of the type of sand on the fracture and mechanical properties of sand concrete. *Advances in Concrete Construction*. 2014;2(1): 13-27. <https://doi.org/10.12989/acc2014.2.1.013>
- [29] Hao Z, Zhe X, Yuying S, Lijuan L, Qiu Y, Xiaozhou Z, Bing C, Dongen C, Feng L, Yidong J. The Early mechanical performance of glass fiber-reinforced manufactured sand concrete. *Journal of Building Engineering*. 2024;83:108440. <https://doi.org/10.1016/j.jobe.2024.108440>
- [30] Konstantoni C, Paneda EM, Biscontin G, Flek NA. The Fracture of bio-cemented sands. *Extreme Mechanics Letters*. 2023;64:102086. <https://doi.org/10.1016/j.eml.2023.102086>
- [31] Mingming Z, Jin XML, Xiapsa Y. The Influence of Stone Powder Content from Manufactured Sand Concrete on Shrinkage, Cracking, Compressive Strength. *Buildings*. 2023; 13(7), 1833. <https://doi.org/10.3390/buildings13071833>

- [32] Hashimoto R, Onoue K. The Crack Resistance of Concrete Using Granulated Blast Furnace Slag Sand under Flexural Stress. Proceeding in Civil Engineering. 21st Ibausil International Conference on Building Materials, Ibausil, 825-832, 2023. <https://doi.org/10.1002/cepa.2832>
- [33] Davim JP. Computational Methods and Production Engineering. Woodhead Publishing Reviews: Mechanical Engineering Series Elsevier, 2017, ISBN 978-0-85709-481-0.
- [34] Davim JP. Design of Experiments in Production Engineering. Springer, 2016, ISBN 978-3-319-23838-8.
- [35] The ASTM C192/192M dealing with the Standard Practice for Making and Curing Concrete Test Specimens in the Laboratory
- [36] The ASTM C293/C293M "Standards Test methods for flexural strength of Concrete (using simple beams with third point loading)".
- [37] Davim JP. Statistical and Computational Techniques in Manufacturing. Springer, 2012, ISBN 978-3-642-25859-6.
- [38] Xianggui Q. Statistical properties of Rechtschaffner designs. Journal of Statistical Planning and Inference. 2007; 137 (7): 2156 - 2164. <https://doi.org/10.1016/j.jspi.2006.06.042>